JOC Article

# Structure-Directed Reversion in the π-Facial Stereoselective Alkylation of Chiral Bicyclic Lactams

Ignacio Soteras,[†] Oscar Lozano,[‡] Carmen Escolano,[‡] Modesto Orozco,[§] Mercedes Amat,[‡] Joan Bosch,*,[‡] and F. Javier Luque*,[†]

Department of Physical Chemistry and Laboratory of Organic Chemistry, Faculty of Pharmacy, and Institute of Biomedicine (IBUB), University of Barcelona, 08028 Barcelona, Spain, Molecular Modeling and Bioinformatics Unit, Institute of Biomedical Research, Barcelona Scientific Park, 08028 Barcelona, Spain, Department of Life Sciences, Barcelona Supercomputing Centre, 08034 Barcelona, Spain, and Department of Biochemistry, Faculty of Biology, University of Barcelona, Barcelona 08028, Spain

fjluque@ub.edu; joanbosch@ub.edu

Received July 29, 2008

exo-b   *endo-a*
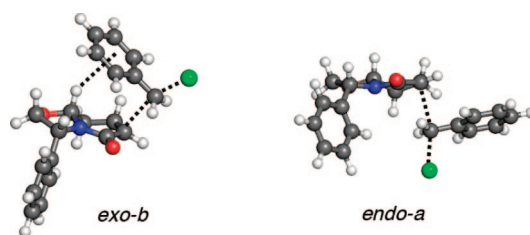
The reversal of the π-facial diastereoselectivity observed in the benzyl bromide alkylation of the enolate of phenylglycinol-derived oxazolopiperidone is examined by means of theoretical calculations and experimental assays. When the angular carbon adopts an *R* configuration, the *endo* addition is intrinsically favored due to the lower torsional strain induced in the TS, but for the reaction with benzyl bromide, which affords the *exo* product. This reversal is attributed to the formation of a C−H···π hydrogen bond between the C−H unit of the C8a angular position and the benzene ring of the alkylating reagent. A similar secondary interaction explains the stereochemical reversion observed in the benzyl alkylation of the enolate of oxazolopyrrolidinone. These findings point out that the delicate balance between factors that dictate the diastereoselectivity in the alkylation of chiral bicyclic lactams can be unexpectedly altered by weak secondary interactions. The results presented here provide valuable guidelines to tune the selective preparation of enantiopure bioorganic and pharmaceutical compounds.

Introduction

The alkylation of enolates generated from chiral bicyclic lactams is a useful method of carbon−carbon bond formation involving the generation of new stereogenic centers, which is highly relevant in the asymmetric synthesis of complex molecules.[1] Meyers and co-workers, in their pioneering and extensive work in this field, demonstrated that the double alkylation of chiral bicyclic [3.3.0] lactams **A** (Scheme 1) is a powerful tool to generate quaternary stereocenters with excellent

SCHEME 1
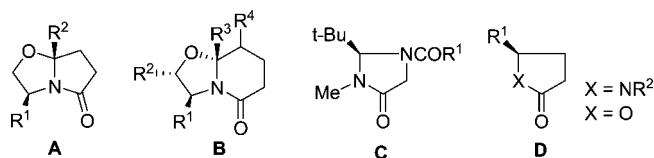
control over the absolute stereochemistry.[2] However, the *endo*:*exo* diastereofacial selectivity is largely dependent on both the nature of the fused ring and the presence of substituents.[3] A similar sensitivity in the stereochemical alkylation outcome has also been reported for bicyclic [4.3.0] lactams **B**.[4] The finding

(2) For reviews, see: (a) Romo, D.; Meyers, A. I. *Tetrahedron* **1991**, *47*, 9503. (b) Meyers, A. I. In *Stereocontrolled Organic Synthesis*; Blackwell Scientific Publications: Oxford, 1994; pp 145−175. (c) Meyers, A. I.; Brengel, G. P. *Chem. Commun.* **1997**, 1. (d) Groaning, M. D.; Meyers, A. I. *Tetrahedron* **2000**, *56*, 9843.

that highly stereoselective alkylations occur in monocyclic imidazolidinone **C**, lactam **D** (X = NR^2), and lactone **D** (X = O) enolates is even more intriguing,[5] because it suggests that factors other than the steric hindrance in the concave-convex faces of the enolate can play an important role.

The nature of the factors that explain the π-facial stereoselectivity in the above alkylations is still a challenging question. For the enolate of imidazolidinone **C**, the involvement of stereoelectronic effects based on the pyramidalization on the C5 carbon has been proposed.[5b] The diastereofacial selectivity in **D** (X = NR^2) has, nevertheless, been ascribed to the competition between the *anti*-stereoelectronic directing effect of the nitrogen lone pair and steric factors[6] or alternatively to the chelation of the enolate by the metal (lithium) ion.[7] In contrast, Houk and co-workers have rationalized the stereochemical selectivity of **D** (X = NR^2) from the differences in the torsional strain in the transition states leading to *endo* and *exo* products.[8] This factor has also been used to explain the stereoselective alkylation of 4-substituted γ-butyrolactones **D** (X = O).[9] Taken together, these results highlight the extreme sensitivity of the stereochemical outcome to apparently minor chemical modifications, which affect the interplay between different factors.

We have recently examined the origin of the π-facial stereoselectivity in the alkylation of the enolates of oxazolopiperidones **1** and **2**,[10] which stems from a delicate balance between torsional strain and steric hindrance. Thus, the diastereoselectivity in **1** is dictated by the greater intermolecular steric hindrance between the incoming alkylating reagent and the piperidone ring of the enolate in the *endo* transition state. However, when the stereocenter at the angular position adopts an *R* configuration (**2**), the phenyl ring at position 3 forces the *pseudo*-planarity of the bicyclic lactam, and the diastereoselectivity is dictated by the internal torsional strain induced in the transition state, leading preferentially to the *endo* product.

TABLE 1. Alkylation of Oxazolopiperidone Lactams 1 and 2

R^2	**1a** *endo:exo*	**1b** *endo:exo*	**2a** *endo:exo*	**2b** *endo:exo*
Me	15:85	5:95	76:24	71:29
Et	0:100		68:32	
CH$_2$CO$_2$tBu	32:68	23:77	88:12	83:17
CH$_2$CH=CH$_2$	10:90	17:83	48:52	48:52
CH$_2$C$_6$H$_5$	23:77	31:69	8:92	10:90

Whereas the preceding rationale justifies the *exo* diastereoselectivity observed for the alkylation of **1** using a variety of reagents (alkyl halides, allyl bromide, or benzyl bromide), this is not true for **2**, since the *endo* preference observed in the enolate alkylation with alkyl halides is completely reversed with benzyl bromide (see Table 1).[11]

The reversal in the facial selectivity, or at least notable changes in the diastereomeric ratio, observed in lactam enolate alkylations when using benzyl bromide instead of alkyl halides has been noted in previous studies, including [3.3.0] lactams, and attributed to steric or mechanistic (SN$_1$ versus SN$_2$) factors.[12,13] However, no theoretical studies devoted to rationalizing the anomalous behavior of benzyl bromide have been reported so far. The aim of this work is to identify the origin of the π-facial stereoselective reversion observed in the benzyl alkylation of bicyclic lactams. To this end, the results of theoretical and experimental studies performed for the benzyl alkylation of the oxazolopiperidone **2** and its 8a-substituted analog **3** and the oxazolopyrrolidinone **4** will be discussed.

Results and Discussion

Stereoselective Alkylation of the Enolate of Oxazolopiperidone 2a. To investigate the origin of the π-facial selectivity reversion observed in the benzylation of the enolate of **2a** (see Table 1), the transition states (TS) leading to *endo* and *exo* additions were located. Two TSs were identified for the *exo* attack, but only one was identified for the *endo* addition (Figure 1). The distance from the benzyl carbon atom in benzyl chloride (denoted C$_b$ hereafter) to the nucleophilic carbon atom (C$_\alpha$) of the enolate was similar in all the TSs (∼2.68 Å).

(3) (a) Roth, G. P.; Leonard, S. F.; Tong, L. *J. Org. Chem.* **1996**, *61*, 5710. (b) Meyers, A. I.; Seefeld, M. A.; Lefker, B. A. *J. Org. Chem.* **1996**, *61*, 5712. (c) Meyers, A. I.; Seefeld, M. A.; Lefker, B. A.; Blake, J. F.; Williard, P. G. *J. Am. Chem. Soc.* **1998**, *120*, 7429. (d) Bailey, J. H.; Byfield, A. T. J.; Davis, P. J.; Foster, A. C.; Leech, M.; Moloney, M. G.; Müller, M.; Prout, C. K. *J. Chem. Soc., Perkin Trans. 1* **2000**, 1977, and references therein. (e) Oda, K.; Meyers, A. I. *Tetrahedron Lett.* **2000**, *41*, 8193. (f) Anwar, M.; Bailey, J. H.; Dickinson, L. C.; Edwards, H. J.; Goswami, R.; Moloney, M. G. *Org. Biomol. Chem.* **2003**, *1*, 2364.

(4) (a) Reeder, M. R.; Meyers, A. I. *Tetrahedron Lett.* **1999**, *40*, 3115. (b) Hughes, R. C.; Dvorak, C. A.; Meyers, A. I. *J. Org. Chem.* **2001**, *66*, 5545. (c) Amat, M.; Escolano, C.; Lozano, O.; Bosch, J. *Org. Lett.* **2003**, *5*, 3139. (d) Amat, M.; Lozano, O.; Escolano, C.; Molins, E.; Bosch, J. *J. Org. Chem.* **2007**, *72*, 4431.

(5) (a) Tomioka, K.; Cho, Y.-S.; Sato, F.; Koga, K. *J. Org. Chem.* **1988**, *53*, 4094. (b) Baldwin, J. E.; Miranda, T.; Moloney, M. *Tetrahedron* **1989**, *45*, 7459. (c) Seebach, D.; Maetzke, T.; Petter, W.; Klötzer, B.; Plattner, D. A. *J. Am. Chem. Soc.* **1991**, *113*, 1781. (d) Ezquerra, J.; Pedregal, C.; Rubio, A.; Yruretagoyena, B.; Escribano, A.; Sánchez-Ferrando, F. *Tetrahedron* **1993**, *49*, 8665. (e) Breña-Valle, L. J.; Carreón, R.; Cruz-Almanza, R. *Tetrahedron: Asymmetry* **1996**, *7*, 1019. (f) Charrier, J.-D.; Duffy, J. E. S.; Hitchcock, P. B.; Young, D. W. *Tetrahedron Lett.* **1998**, *39*, 2199. (g) Maldaner, A. O.; Pilli, R. A. *Tetrahedron* **1999**, *55*, 13321.

(6) (a) Meyers, A. I.; Seefeld, M. A.; Lefker, B. A.; Blake, J. F. *J. Am. Chem. Soc.* **1997**, *119*, 4565. (b) Meyers, A. I.; Seefeld, M. A.; Lefker, B. A.; Blake, J. F.; Williard, P. G. *J. Am. Chem. Soc.* **1998**, *120*, 7429.

(7) (a) Durkin, K. A.; Liotta, D. *J. Am. Chem. Soc.* **1990**, *112*, 8162. (b) Ikuta, Y.; Tomoda, S. *Tetrahedron Lett.* **2003**, *44*, 5931. (c) Ikuta, Y.; Tomoda, S. *Org. Lett.* **2004**, *6*, 189.

(8) Ando, K.; Green, N. S.; Li, Y.; Houk, K. N. *J. Am. Chem. Soc.* **1999**, *121*, 5334.

(9) Ando, K. *J. Am. Chem. Soc.* **2005**, *127*, 3964.

(10) (a) Soteras, I.; Lozano, O.; Gómez-Esqué, A.; Escolano, C.; Orozco, M.; Amat, M.; Bosch, J.; Luque, F. J. *J. Am. Chem. Soc.* **2006**, *128*, 6581. (b) For a recent review on chiral oxazolopiperidone lactams, see: Escolano, C.; Amat, M.; Bosch, J. *Chem. Eur. J.* **2007**, *72*, 4431.

(11) Amat, M.; Escolano, C.; Lozano, O.; Gómez-Esqué, A.; Griera, R.; Molins, E.; Bosch, J. *J. Org. Chem.* **2006**, *71*, 3804.

(12) (a) Schwarz, J. B.; Meyers, A. I. *J. Org. Chem.* **1998**, *63*, 1619. (b) Mills, C. E.; Heightman, T. D.; Hermitage, S. A.; Moloney, M. G.; Woods, G. A. *Tetrahedron Lett.* **1998**, *39*, 1025. (c) Zhang, R.; Brownewell, F.; Madalengoitia, J. S. *Tetrahedron Lett.* **1999**, *40*, 2707. (d) Brewster, A. G.; Broady, S.; Davies, C. E.; Heightman, T. D.; Hermitage, S. A.; Hughes, M.; Moloney, M. G.; Woods, G. *Org. Biomol. Chem.* **2004**, *2*, 1031. See also refs 3d and 5e.

(13) (a) Armstrong, R. W.; DeMattei, J. A. *Tetrahedron Lett.* **1991**, *32*, 5749. (b) Beard, M. J.; Bailey, J. H.; Cherry, D. T.; Moloney, M. G.; Shim, S. B.; Statham, K. A. *Tetrahedron* **1996**, *52*, 3719.
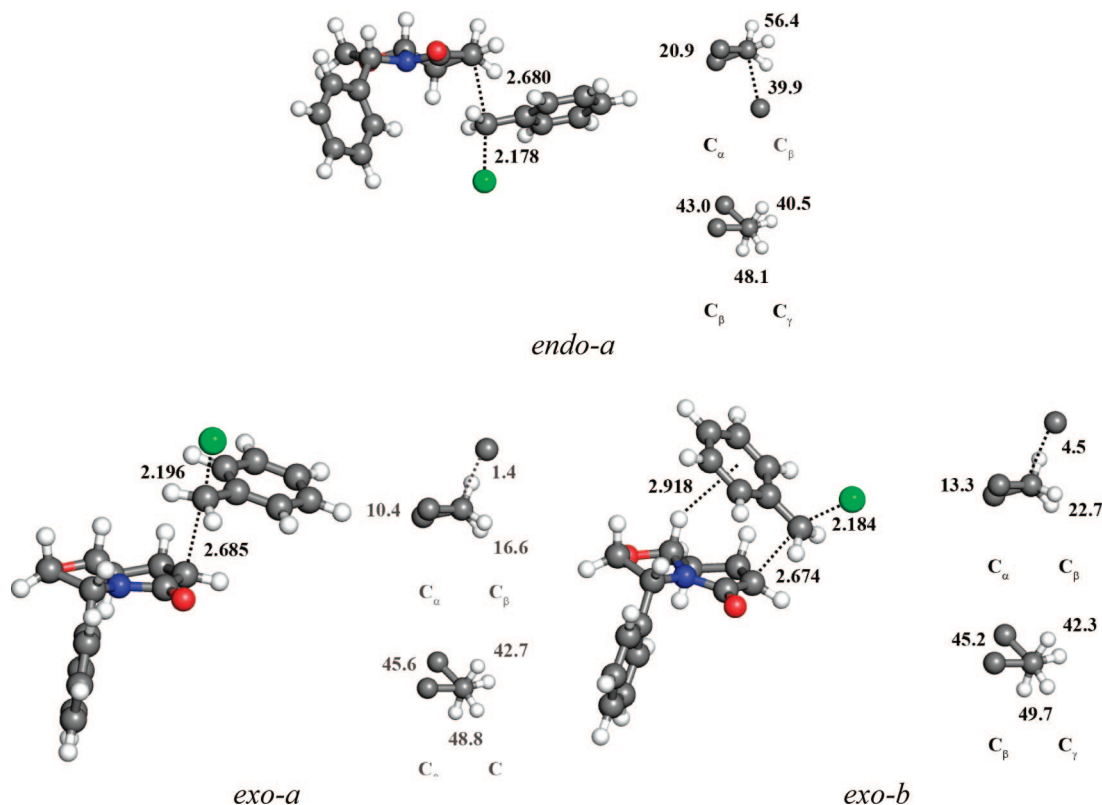
endo-a

exo-a

exo-b

FIGURE 1. Transition state structures for the *endo* (top) and *exo* (bottom) addition of benzyl chloride to the enolate of oxazolopiperidone **2a**, together with the Newman projections viewed from the directions along the $C_\alpha-C_\beta$ and $C_\beta-C_\gamma$ bonds (the forming bond between C_α and C_b is shown by a dotted line in Newman projections). Distances and torsional angles are in angstroms and degrees, respectively.

TABLE 2. Gibbs Free Energy Differences (at 298 K; kcal/mol) between *endo* and *exo* Transition States for Addition of Benzyl Chloride to the Enolate of Oxazolopiperidone 2a

solvent	*endo-a*	*exo-a*	*exo-b*
gas[a]	2.5 (3.1)	4.0 (4.8)	0.0 (0.0)
	3.3 (3.8)	4.7 (5.4)	0.0 (0.0)
	2.5 (3.0)	2.9 (4.7)	0.0 (0.0)
carbon tetrachloride	2.6	4.0	0.0
chloroform	2.7	3.8	0.0
octanol	2.2	3.7	0.0
water	2.6	3.1	0.0

[a] Relative stabilities in the gas phase determined at the (top) MP2/6-31+G(d), (middle) MP2/aug-cc-pVDZ, and (bottom) composite MP2/aug-cc-pVDZ + (CCSD-MP2)/6-31G(d) levels. This latter value was used to obtain the relative stabilities in solution. The relative energies corrected by zero-point energies are given in parentheses.

The *endo* TS is destabilized relative to the *exo* (*exo-b* TS) attack by 2.5 kcal/mol in the gas phase (Table 2). The origin of such an stabilization is mainly due to dispersion, as the two TSs have similar energies at the Hartree–Fock level (energy differences of −0.1 and 0.8 kcal/mol for *endo* and *exo-a* relative to *exo-b*). In agreement with our previous studies,[10a] such a difference in stability is little affected upon solvation. At first sight, the destabilization of the *endo* TS is surprising, since the Newman projection along the enolate carbon atoms $C_\alpha-C_\beta$ (Figure 1) indicates that the torsional strain is lower in the TS leading to the *endo* product, as already noted for the attack of alkyl halides.[10a] Nevertheless, the preferential stability of the *exo-b* TS can be realized from the secondary interaction between the C−H unit at the angular 8a-position and the benzene ring of the attacking group, where the C−H is pointing toward the center of the benzene

SCHEME 2
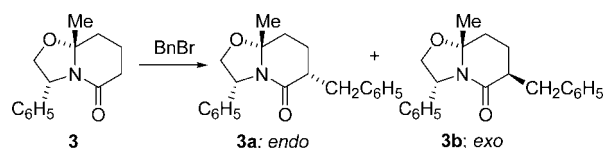
ring (distance of 2.92 Å; Figure 1). Such a C−H···π hydrogen bond, which is mainly stabilized by dispersion forces,[14] is topologically reflected in the formation of a cage critical point in the electron density ($\rho_{cage} = 0.0030$ au), as already noted in the complexation of benzene with CH_4.[15]

To corroborate the role of the C−H···π hydrogen bond, the reaction with benzyl bromide was performed with the enolate of the substituted oxazolopiperidone **3**, which bears an additional methyl group at the angular position. According to our hypothesis, such a chemical modification would prevent the formation of the C−H···π interaction and sterically destabilize the *exo-b* TS shown in Figure 1. As expected, the *cis* relationship found between the hydrogen atoms at positions 3 and 6 from the NMR data (see Supporting Information) confirmed that the major product corresponds to the *endo* alkylation (**3a**:**3b** 70:30) (Scheme 2). To further explore our hypothesis, additional reactions were performed for *p*-nitro and *p*-methoxy derivatives of benzyl bromide. When the alkylation of oxazolopiperidone **2a** was performed with *p*-methoxybenzyl bromide, only the

(14) (a) Hobza, P.; Spirko, V.; Selzle, H. L.; Schlag, E. W. *J. Phys. Chem. A* **1998**, *102*, 2501. (b) Hobza, P.; Spirko, V.; Havlas, Z.; Buchhold, K.; Reimann, B.; Barth, H. D.; Brutschy, B. *Chem. Phys. Lett.* **1999**, *299*, 180. (c) Cubero, E.; Orozco, M.; Hobza, P.; Luque, F. J. *J. Phys. Chem. A* **1999**, *103*, 6394.
(15) Cubero, E.; Orozco, M.; Luque, F. J. *J. Phys. Chem. A* **1999**, *103*, 315.
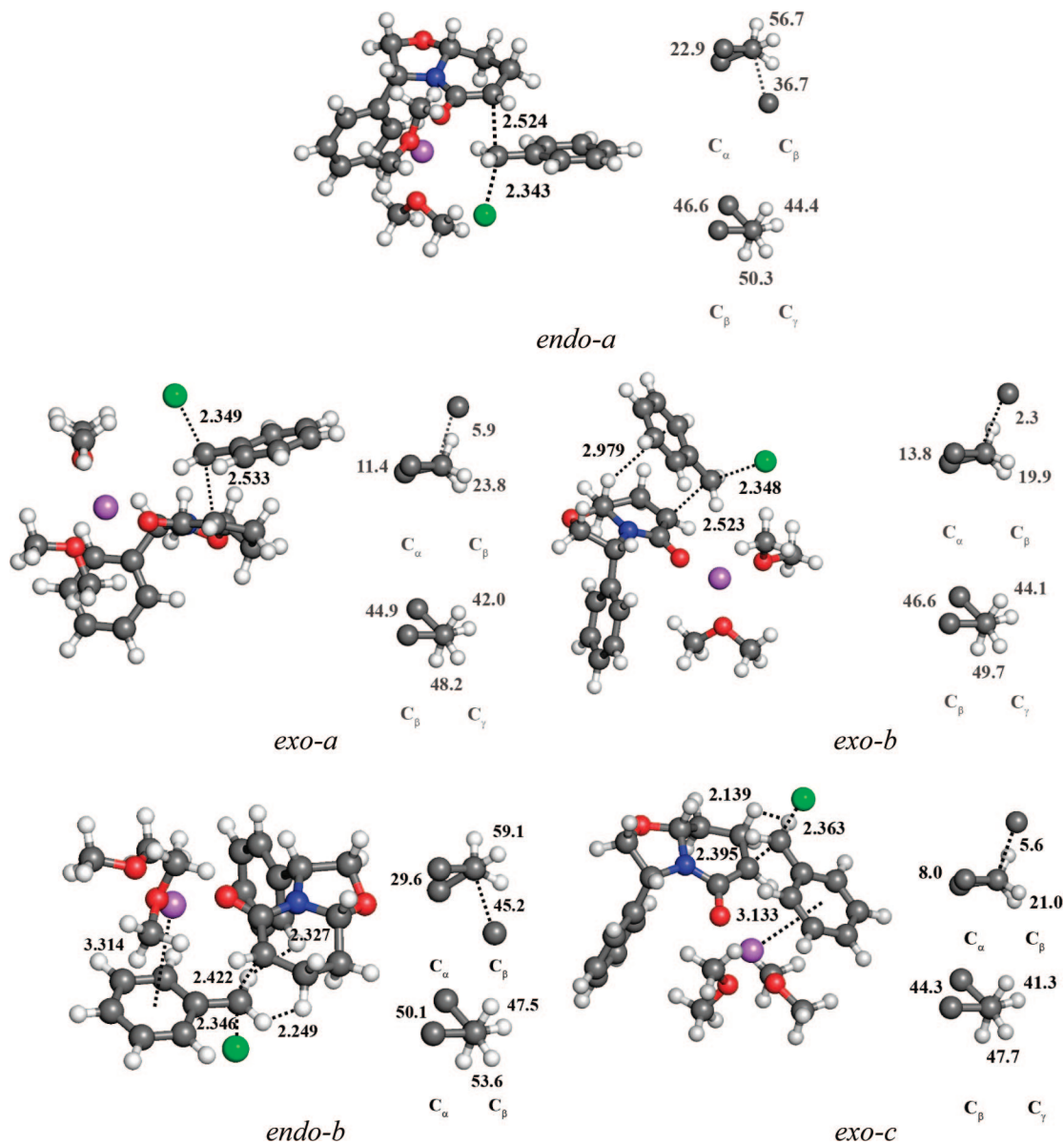
FIGURE 2. Transition state structures for the *endo* (top) and *exo* (bottom) addition of benzyl chloride to the enolate of oxazolopiperidone **2a** coordinated to a Li$^+$ cation, together with the Newman projections viewed from the directions along the $C_\alpha-C_\beta$ and $C_\beta-C_\gamma$ bonds (the forming bond between C_α and C_b is shown by a dotted line in Newman projections). Distances and torsional angles are in angstroms and degrees, respectively.

exo isomer was detected. In contrast, the alkylation of **2a** with *p*-nitrobenzyl bromide afforded a 2:3 mixture of *endo/exo* isomers, thus suggesting that the presence of an electron-withdrawing group on the benzyl moiety results in a less effective C−H···π interaction. Overall, present results suggest that the intrinsic diastereoselectivity preference in the alkylation of the enolate of **2a**, which would favor the *endo* addition due to the larger torsional strain in the *exo* TS, is reverted when the alkylating reagent is benzyl due to the formation of the secondary C−H···π interaction.

Several studies have suggested that coordination with Li$^+$ cation might affect the stereochemical outcome in Meyers-type enolate alkylations.[7] Nevertheless, the potential influence exerted by Li$^+$ coordination is not supported by the experimental results reported by Romo and Meyers[2a] nor by theoretical studies recently reported by Ando[9] for the stereoselective alkylation of γ-butyrolactones enolates. Simi-

lar conclusions were found in our previous studies about the stereoselective alkylation of the enolate of **2a**.[10a] However, because cation−π interactions are strongly stabilizing,[16] we decided to further explore whether Li$^+$ coordination to the enolate or to the benzyl group might affect the stereochemical outcome.

The structures of the TSs corresponding to the addition of benzyl chloride to the enolate of **2a** coordinated to a Li$^+$ cation were located (Figure 2). Due to computational limitations, dimethyl ether was used to mimic two solvating

(16) (a) Ma, J.; Dougherty, D. A. *Chem. Rev.* **1997**, *97*, 1303. (b) Cubero, E.; Luque, F. J.; Orozco, M. *Proc. Natl. Acad. Sci. U.S.A.* **1998**, *95*, 5976. (c) Tsuzuki, S.; Yoshida, M.; Uchimaru, T.; Mikami, M. *J. Phys. Chem. A* **2001**, *105*, 769. (d) Reddy, A. S.; Zipse, H.; Sastry, G. N. *J. Phys. Chem. B* **2007**, *111*, 11546.

(17) (a) McKeever, L. D.; Waack, R.; Doran, M. A.; Baker, E. B. *J. Am. Chem. Soc.* **1969**, *91*, 1057. (b) Bauer, W.; Winchester, W. R.; Schleyer, P. V. R. *Organometallics* **1987**, *6*, 2371.

TABLE 3. Gibbs Free Energy Differences (at 298 K; kcal/mol) between *endo* and *exo* Transition States for Addition of Benzyl Chloride to the Enolate of Li⁺-Coordinated Oxazolopiperidone 2a

method[a]	endo-a	endo-b	exo-a	exo-b	exo-c
MP2/6-31+G(d)	2.8 (2.9)	1.2 (0.7)	3.8 (4.6)	0.0 (0.0)	3.4 (3.0)
MP2/6-311++(d,p)	2.9 (3.0)	1.2 (0.7)	4.2 (5.1)	0.0 (0.0)	3.5 (3.2)

[a] The relative electronic energies corrected by zero-point energies in the gas phase are given in parentheses.

THF molecules, as done previously by Ando.[9] Moreover, even though several aggregation states have been described for alkyl lithiums in THF, there is a tendency to form monomers as the size of the coordinating alkyl group is enlarged.[17] For instance, whereas methyl lithium is found to be tetrameric in THF, *tert*-butyl lithium is a monomer. Accordingly, for our purposes here, a model system formed by direct coordination of solvated Li⁺ cation to the enolate of the oxazolopiperidone seems plausible.

The same TSs (*endo-a*, *exo-a*, and *exo-b*) shown in Figure 1 were identified in the structures optimized for the Li⁺-coordinated TSs (Figure 2). The major differences are the shortening of the C_α–C_b bonds by 0.11–0.16 Å (C_α–C_b distances of ∼2.53 Å), and the lengthening of the C_b–Cl bond by 0.16–0.19 Å. Moreover, the *exo-b* TS retains the C–H···π hydrogen bond (distance to the benzene ring of 2.98 Å), but pointing toward one of the benzene carbon atoms, leading to the formation of a bond critical point (ρ_{bond} = 0.0074 au).
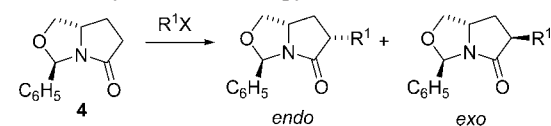
In addition, two new TSs where Li⁺, besides interacting with the carbonyl oxygen of the enolate, forms a cation···π interaction with the benzene ring of the incoming reactant were located (*endo-b* and *exo-c* in Figure 2). Compared to the preceding TSs, the length of the C_α–C_b bond is shorter (*endo-b* 2.42 Å; *exo-c* 2.40 Å), while the length of the C_b–Cl bond is mostly unaffected (*endo-b* 2.35 Å; *exo-c* 2.36 Å). The distance of the Li⁺ cation to the center of the benzene ring (*endo-b* 3.31 Å; *exo-c* 3.13 Å) is much larger than the value optimized for the benzene···Li⁺ complex (1.94 Å at the MP2/6-311++G(d,p) level).[16d] This finding, in conjunction with the fact that Li⁺ deviates notably from the normal to the ring, suggests that the cation···π interaction is weak, as expected from the dominant contribution played by the electrostatic attraction with the negative charge of the enolate.

The relative stabilities of the *endo-a*, *exo-a*, and *exo-b* TSs are little affected by Li⁺ coordination (Table 3) and reflect the values reported in Table 2. Moreover, the *endo-b* and *exo-c* TSs are destabilized with regard to the *exo-b* TS by 1.2 and 3.4 kcal/mol, respectively, which can be attributed to repulsive contacts between the benzylic CH_2 unit and hydrogen atoms of the enolate (see Figure 2). Overall, the results point out that the *exo-b* TS is the preferred route for the addition of benzyl chloride to the enolate of oxazolopiperidone **2a**.

To further check the preceding conclusion, the stereochemical outcome in the reaction of the enolate of lactam **2a** with benzyl bromide was experimentally examined under different conditions in order to explore the effect of solvent (THF vs toluene), cation (Li⁺ vs K⁺), and cosolvent (HMPA) on the diastereomeric *endo:exo* ratio. The results (Table 4) demonstrate that the use of KHMDS as the base instead of LiHMDS or the addition of HMPA did not change the ratio of the final products, while performing the reaction in toluene

TABLE 4. Alkylation of Oxazolopiperidone Lactam 2a under Different Experimental Conditions

entry	base	solvent	cosolvent	endo:exo
1	LiHMDS	THF		1:9
2	LiHMDS	toluene		3:7
3	LiHMDS	THF	HMPA	1:9
4	KHMDS	toluene		3:7
5	KHMDS	THF		1:9

TABLE 5. Alkylation of Oxazolopyrrolidinone Lactam 4

R¹	endo:exo
Me	5:1;[13a] 2.9:1[13b]
CH₂C₆H₅	1:2;[13a] 1:2.1[13b]

merely resulted in a change in the *endo:exo* ratio (3:7), the major isomer again being the *exo* product.

In summary, both theoretical and experimental results indicate that the diastereomeric reversal observed for the reaction with benzyl chloride reflects intrinsic differences in the TSs leading to *endo* and *exo* products related to the formation of weak C–H···π interactions. Both experimental and theoretical studies of the benzene-methane cluster in the gas phase indicate that the complexation energy amounts to −1.1 kcal/mol.[18] Even though this is a modest contribution, the relative stability found between the *endo* and *exo* TSs corresponding to the methyl alkylation of **2a** was estimated to be less than 1 kcal/mol.[10a] Accordingly, the formation of a C–H···π bond in the benzyl alkylation of the enolates of oxazolopiperidones has a direct role in modulating the π-facial stereoselective outcome.

Stereoselective Alkylation of the Pyrrolidinone Enolate 4. The dramatic effect of a benzyl alkylating group on the stereoselectivity of enolate alkylations has also been noticed experimentally for the enolate of oxazolopyrrolidinone **4** (Table 5).[13] It might then be speculated that the structure-directed π-facial reversion mechanism reported above for the benzyl addition to the enolate of oxazolopiperidone **2a** could also operate for the pyrrolidinone enolate. To verify this hypothesis, computations were also performed to locate the TSs for the alkylation of the pyrrolidinone ring.

Three and two TSs were identified for the *endo* and *exo* additions, respectively (Figure 3). The C_α–C_b distance varies from 2.58 to 2.61 Å in both *endo* and *exo* TSs. According to the Newman projections along the enolate carbon atoms C_α–C_β, there is larger torsional strain in the TS leading to the *exo* product, which would therefore favor the *endo* addition. However, comparison of the relative stabilities between TSs (Table 6) indicates that the most favorable benzylation occurs at the *exo* face, the *endo* addition being destabilized by 1.6 kcal/mol. Inspection of the optimized structures reveals the formation of C–H···π interactions in both *endo-c* (ρ_{cage} = 0.0041 au) and *exo-a* (ρ_{bond} = 0.0084 au) TSs, which involve hydrogens of the C-2 and C-7 methylene groups, respectively. The former TS, however, is destabilized by 2.0 kcal/mol relative to the *exo-a* TS, as

(18) Shibasaki, K.; Fujii, A.; Mikami, N.; Tsuzuki, S. *J. Phys. Chem. A* **2006**, *110*, 4397.
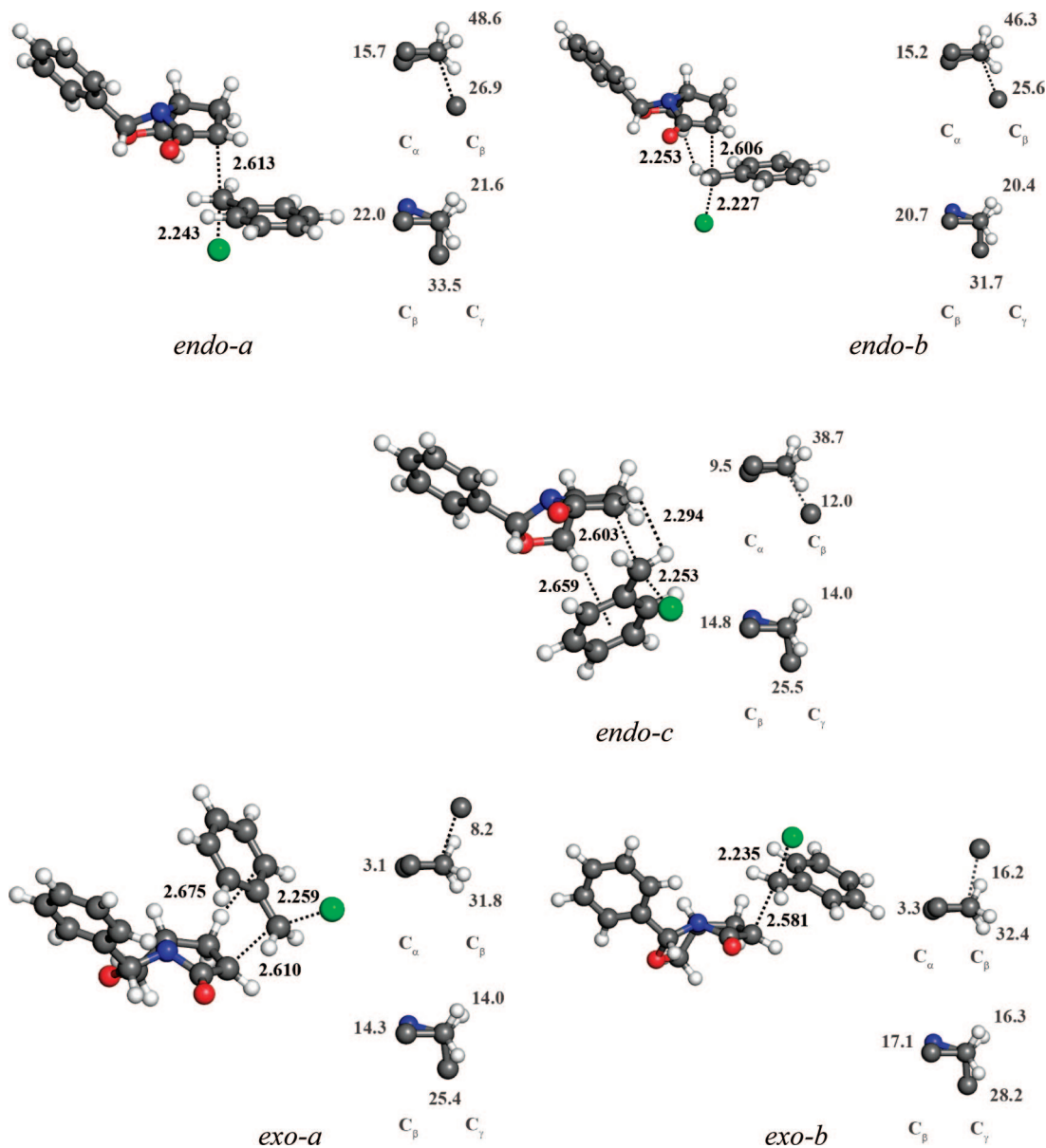
FIGURE 3. Transition structures for the *endo* and *exo* addition of benzyl chloride to the enolate of pyrrolidinone **4**, together with the Newman projections viewed from the directions along the C_α–C_β and C_β–C_γ bonds (the forming bond between C_α and C_b is shown by a dotted line in theNewman projections). Distances and torsional angles are in angstroms and degrees, respectively.

TABLE 6.   Gibbs Free Energy Differences (at 298 K; kcal/mol) between *endo* and *exo* Transition States for Addition of Benzyl Chloride to the Enolate of Pyrrolidinone 4

method[a]	endo-a	endo-b	endo-c	exo-a	exo-b
MP2/6-31+G(d)	3.1 (3.6)	1.8 (2.8)	2.6 (2.6)	0.0 (0.0)	1.4 (1.9)
MP2/aug-cc-pVDZ	4.1 (4.5)	2.3 (3.2)	2.8 (2.7)	0.0 (0.0)	1.8 (2.3)
MP2/aug-cc-pVDZ + (CCSD-MP2)/6-31G(d)	2.9 (3.4)	1.6 (2.7)	2.0 (1.9)	0.0 (0.0)	1.5 (2.0)

[a] The relative electronic energies corrected by zero-point energies in the gas phase are given in parentheses.

expected from the more crowded structure of the *endo-c* TS, which is in fact slightly less stable than the *endo-b* TS (see Table 6).

(19) Frontera, A.; Garau, C.; Quiñonero, D.; Ballester, P.; Costa, A.; Deyà, P. M. *Org. Lett.* **2003**, *5*, 1135.

Conclusion

Previous studies have shown that C–H···π interactions modulate the diastereselectivity of host–guest complexes.[19] The results presented here demonstrate that the reversion of the π-facial selectivity observed experimentally in the benzyl bromide alkylation of the enolates of both ozaxolopiperidone **2a** and oxazolopyrrolidinone **4** can be attributed to the formation of a C–H···π bond between the enolate and the benzene ring of the incoming reagent. Whereas in **2a** such an interaction involves the C–H unit of the C8a angular position, the stereochemical reversion observed in **4** is due to the interaction with one of the C-7 methylene hydrogens. Therefore, the subtle balance among different factors that mediate the stereochemical outcome in the alkylation of chiral bicyclic [4.3.0] and [3.3.0] lactams can be altered by unexpected weak secondary interactions. These findings may

provide useful guidelines to tune the selective preparation of enantiopure derivatives, which is a crucial aspect in the design of bioorganic and pharmaceutical compounds.

Experimental Section

Computational Details. The computational protocol used here follows the main trends adopted in our previous study about the origin of the π-facial stereoselectivity in the methyl alkylation of the enolates of oxazolopiperidones **1** and **2**.[10a] On the basis of previous studies,[10a,20] which showed that single point MP2 energies at the B3LYP geometries provide a reasonable estimate of the lithium enolate activation barrier, full geometry optimizations were performed with the B3LYP[21] density functional method using the 6-31+G(d) basis set, and single-point MP2/6-31+G(d) and MP2/aug-cc-pVDZ calculations were subsequently performed to determine the relative energies of the *endo* and *exo* transition states. Higher-order electron correlation effects were estimated from CCSD/6-31G(d) calculations, and the best estimate of the energy difference between transition states was determined by combining the relative energies computed at the MP2/aug-cc-pVDZ level and the energy correction obtained from CCSD and MP2 calculations performed with the 6-31G(d) basis set [denoted in the following as MP2/aug-cc-pVDZ + (CCSD-MP2)/6-31G(d)]. The nature of the stationary points was verified by inspection of the vibrational frequencies, which were used to calculate zero point, thermal and entropic corrections within the framework of the harmonic oscillator-rigid rotor at 1 atm and 298 K. These corrections were added to the electronic energies to estimate the free energy differences in the gas phase.

The relative stabilities in solution were estimated by combining the free energy difference in the gas phase and the differences in solvation free energy determined from MST calculations.[22] QM SCRF continuum calculations were performed by using the B3LYP/6-31G(d) optimized version of the MST(IEF) model,[23] which relies on the integral equation formalism (IEF)[24] of the polarizable continuum model.[25] The MST model determines the solvation free energy by three terms, which account for electrostatic, cavitation, and van der Waals contributions associated with the transfer of the solute from the gas phase to solution. Since the MST model has not been parametrized to treat solvation in tetrahydrofuran (i.e., the solvent used in experimental assays; see below),[26] calculations were performed for the solvation in water, octanol, chloroform and carbon tetrachloride in order to explore the effect of varying the polarity of the solvent.[23,27]

Gas phase calculations were carried out using Gaussian03.[28] MST calculations were performed using a locally modified version of Gaussian-03.

Experimental Procedures. The generation of the enolate of **2a** was carried out at low temperature (−78 °C) for 1 h using lithium bis(trimethylsilyl)amide (1 M in THF, 1.5 equiv) as the base, followed by addition of the alkylating reagent (2.5 equiv). The reaction mixture was then stirred at −78 °C for 2 h and quenched by addition of a saturated aqueous solution of sodium chloride. Reactions were performed using THF as the solvent. Additional experiments were carried out upon lactam **2a** to evaluate the effect that the solvent (THF, toluene), the cation of the base (Li⁺, K⁺), and cosolvent (HMPA, 2 equiv) could have on the diastereomeric *endo*:*exo* ratio.

[3*R*,6*R*(and 6*S*),8a*R*]-6-Benzyl-8a-methyl-5-oxo-3-phenyl-2,3,6,7,8,8a-hexahydro-5*H*-oxazolo[3,2-*a*]pyridine (3a and 3b) and (3*R*,8a*R*)-6,6-Dibenzyl-8a-methyl-5-oxo-3-phenyl-2,3,6,7,8,8a-hexahydro-5*H*-oxazolo[3,2-*a*]pyridine (3c). A solution of the lactam **3**[29] (200 mg, 0.87 mmol) in THF (2 mL) was added to a cooled (−78 °C) solution of LiHMDS (1 M in THF, 1.0 mL, 1.0 mmol) in THF (10 mL). After the solution stirred at −78 °C for 1 h, benzyl bromide (0.15 mL, 1.31 mmol) was added, and stirring was continued for 2 h. The reaction was quenched by the addition of saturated aqueous NaCl, and the resulting mixture was extracted with EtOAc and CH₂Cl₂. The combined organic extracts were dried and concentrated, and the resulting residue was chromatographed (1:1 hexane−EtOAc) to afford a mixture of epimers **3a** and **3b** [165 mg, 59%; (70:30 calculated by GC/MS)], dialkylated product **3c** (50 mg, 14%), and starting lactam **3** (34 mg, 17%). **3a**: IR (film) 1654 cm⁻¹; ¹H NMR (300 MHz) δ 1.34 (s, 3H, CH₃), 1.56 (m, 1H, H-7), 1.72 (m, 1H, H-7), 1.90−1.97 (m, 2H, H-8), 2.39 (m, 1H, H-6), 2.46 (dap, J = 9.6 Hz, 1H, CH₂Ph), 2.99 (dap, J = 9.6 Hz, 1H, CH₂Ph), 3.83 (dd, J = 9.0, 2.0 Hz, 1H, H-2), 4.33 (dd, J = 9.0, 7.0 Hz, 1H, H-2), 4.81 (dd, J = 7.0, 2.0 Hz, 1H, H-3), 6.96−7.22 (m, 10H, ArH); ¹³C NMR (75.4 MHz) δ 21.7 (C-7), 23.8 (CH₃), 32.5 (C-8), 37.1 (CH₂Ph), 40.7 (C-6), 58.8 (C-3), 71.5 (C-2), 93.1 (C-8a), 126.0 (CH), 126.3 (2CH), 127.3 (CH), 128.2 (2CH), 128.4 (2CH), 129.1 (2CH), 139.7 (C *i*), 141.7 (C *i*), 169.4 (NCO); [α]²²_D +43 (*c* 0.9, MeOH); MS-EI *m/z* 321 (M⁺, 43), 306 (100), 187 (12), 162 (39), 120 (92), 91 (89); HMRS calcd for C₂₁H₂₃NO₂ (M⁺ + 1) 322.1801, found 322.1804. **3b**: IR (film) 1647 cm⁻¹; ¹H NMR (300 MHz) δ 1.12 (s, 3H, CH₃), 1.57 (m, 1H, H-7), 1.77−1.91 (m, 2H, H-7, H-8), 2.09 (dt, J = 13.0, 4.0 Hz, 1H, H-8), 2.43 (m, 1H, H-6), 2.79 (dd, J = 13.5, 8.0 Hz, 1H, CH₂Ph), 3.07 (dd, J = 13.5, 4.0 Hz, 1H, CH₂Ph), 3.86 (dd, J = 9.5, 2.0 Hz, 1H, H-2), 4.37 (dd, J = 9.5, 7.5 Hz, 1H, H-2), 4.85 (dd, J = 7.5, 2.0 Hz, 1H, H-3), 7.09−7.26 (m, 10H, ArH); ¹³C NMR (75.4 MHz) δ 23.1 (CH₃), 23.3 (C-7), 34.3 (C-8), 37.3 (CH₂Ph), 42.8 (C-6), 59.2 (C-3), 71.4 (C-2), 93.1 (C-8a), 126.2 (3CH), 127.3 (CH), 128.2 (2CH), 128.5 (2CH), 129.4 (2CH), 139.3 (C *i*), 141.8 (C *i*), 168.6 (NCO); [α]²²_D −129 (*c* 0.58, MeOH); MS-EI *m/z* 321 (M⁺, 34), 306 (100), 187 (12), 162 (30), 120 (82), 91 (84); HMRS calcd for C₂₁H₂₃NO₂ (M⁺ + 1) 322.1801, found 322.1797. **3c**: IR (film) 1642 cm⁻¹; ¹H NMR (300 MHz) δ 0.63 (s, 3H, CH₃), 1.77−1.92 (m, 4H, H-7, H-8), 2.23 (d, J = 12.5 Hz, 1H, CH₂Ph), 2.67 (d, J = 13.5 Hz, 1H, CH₂Ph), 2.94 (d, J = 13.5 Hz, 1H, CH₂Ph), 3.42 (d, J = 12.5 Hz, 1H, CH₂Ph), 3.92 (dd, J = 9.2, 2.2 Hz, 1H, H-2), 4.35 (dd, J = 9.2, 7.2 Hz, 1H, H-2), 4.83 (dd, J = 7.2, 2.2 Hz, 1H, H-3), 6.99−7.02 (m, 3H, ArH), 7.16−7.41 (m, 12H, ArH); ¹³C NMR (75.4 MHz) δ 22.0 (CH₃), 23.7 (C-7), 31.9 (C-8), 42.8 (CH₂Ph), 44.9 (CH₂Ph), 47.8 (C-6), 59.1 (C-3), 71.4 (C-2), 93.1 (C-8a), 126.3 (CH), 126.5 (CH), 126.9 (2CH), 127.3 (CH), 128.0 (4CH), 128.3 (2CH), 131.0 (2CH), 131.0 (2CH), 137.0 (C *i*),

(20) Pratt, L. M.; Van Nguyen, N.; Ramachandran, B. *J. Org. Chem.* **2005**, *70*, 4279.

(21) (a) Becke, A. B. *J. Chem. Phys.* **1993**, *98*, 5648. (b) Becke, A. B. *Phys. Rev. A* **1998**, *38*, 3098. (c) Lee, C.; Yang, W.; Parr, R. G. *Phys. Rev. B* **1988**, *37*, 785.

(22) Since the MST model was parametrized from experimental free energies of solvation at 298 K, the gas phase free energy difference was also determined at this temperature for the sake of internal consistency.

(23) (a) Bachs, M.; Luque, F. J.; Orozco, M. *J. Comput. Chem.* **1994**, *15*, 446. (b) Curutchet, C.; Orozco, M.; Luque, F. J. *J. Comput. Chem.* **2001**, *22*, 1180. (c) Soteras, I.; Curutchet, C.; Bidon-Chanal, A.; Orozco, M.; Luque, F. J. *J. Mol. Struct. (THEOCHEM)* **2005**, *727*, 29.

(24) (a) Cancès, E.; Mennucci, B. *J. Math. Chem.* **1998**, *23*, 309. (b) Cancès, E.; Mennucci, B.; Tomasi, J. *J. Chem. Phys.* **1997**, *107*, 3032. (c) Mennucci, B.; Cancès, E.; Tomasi, J. *J. Phys. Chem. B* **1997**, *101*, 10506.

(25) (a) Miertus, S.; Scrocco, E.; Tomasi, J. *Chem. Phys.* **1981**, *55*, 117. (b) Miertus, S.; Tomasi, J. *Chem. Phys.* **1982**, *65*, 239.

(26) The dielectric permittivity is 7.5 at 295 K. Data taken from *Handbook of Chemistry and Physics*, 80th ed.; Lide, D. R., Ed.; CRC: Boca Raton, 1999.

(27) (a) Orozco, M.; Bachs, M.; Luque, F. J. *J. Comput. Chem.* **1995**, *16*, 563. (c) Luque, F. J.; Zhang, Y.; Aleman, C.; Bachs, M.; Gao, J.; Orozco, M. *J. Phys. Chem.* **1996**, *100*, 4269. (d) Luque, F. J.; Alemán, C.; Bachs, M.; Orozco, M. *J. Comput. Chem.* **1996**, *17*, 806.

(28) Frisch, M. J. et al. *Gaussian 03, Revision B.04*; Gaussian, Inc.: Pittsburgh PA, 2003.

(29) Munchhorf, M. J.; Meyers, A. I. *J. Org. Chem.* **1995**, *60*, 7084.

138.0 (C *i*), 141.9 (C *i*), 170.7 (NCO); $[\alpha]^{22}_D$ −42 (*c* 1.0, MeOH); MS-EI *m/z* 411 (M$^+$, 1), 396 (39), 320 (100), 200 (6), 120 (22), 91 (72); HMRS calcd for $C_{28}H_{29}NO_2$ (M$^+$ + 1) 412.2171, found 412.2265.

Supporting Information Available: Complete ref 22, B3LYP/6-31+G(d) geometries of the transition states for the reaction of enolates derived from **2a** and **4** with benzyl chloride, and copies of the ^{1}H and ^{13}C NMR spectra of compounds **3a**, **3b**, and **3c**. This material is available free of charge via the Internet at http://pubs.acs.org.

JO801665K